Available online at www.sciencedirect.com
ScienceDirect
Cellular Signalling 18 (2006) 1801 – 1812
CELLULAR SIGNALLING
www.elsevier.com/locate/cellsig

Involvement of JNKs and p38-MAPK/MSK1 pathways in H_2O_2-induced upregulation of heme oxygenase-1 mRNA in H9c2 cells

Ioanna-Katerina S. Aggeli, Catherine Gaitanaki, Isidoros Beis *

Department of Animal and Human Physiology, School of Biology, Faculty of Sciences, University of Athens, Panepistimioupolis Ilissia, 157 84 Athens, Greece

Received 10 January 2006; received in revised form 31 January 2006; accepted 3 February 2006

Abstract

One of the most important challenges that cardiomyocytes experience is an increase in the levels of reactive oxygen species (ROS), i.e., during ischemia, reperfusion as well as in the failing myocardium. HOX-1 has been found to protect cells and tissues against oxidative damage; therefore, we decided to study the signalling cascades involved in its transcriptional regulation. HOX-1 mRNA levels were found to be maximally induced after 6 h of treatment with 200 μM H_2O_2 and remained elevated for at least 24 h. Inhibition of JNKs, p38-MAPK and MSK1 pathways, by pharmacological inhibitors, reduced HOX-1 mRNA levels in H_2O_2-treated H9c2 cells. In parallel, we observed that all three subfamilies of the mitogen-activated protein kinases (MAPKs) attained their maximal phosphorylation levels at 5–15 min of H_2O_2 treatment, with mitogen- and stress-activated-protein kinase 1 (MSK1) also being maximally phosphorylated at 15 min. H_2O_2-induced MSK1 phosphorylation was completely abrogated in the presence of the selective p38-MAPK inhibitor SB203580. In an effort to define possible substrates of MSK1, we found that ATF2 as well as cJun phosphorylation were equally induced after 30 min and 60 min, respectively, a response inhibited by SP600125 (JNKs inhibitor) and H89 (MSK1 inhibitor), indicating the involvement of these kinases in the observed response. This finding was further substantiated with the detection of a potential signalling complex composed of either p-MSK1 and p-cJun or p-MSK1 and p-ATF2 (co-immunoprecipitation). ATF2 and cJun are known AP1 components. Given the presence of an AP-1 site in HOX-1 promoter region, the activity of AP1 transcription factor was examined. Electrophoretic mobility shift assays performed showed a maximal upregulation of AP1 binding activity after 60 min of H_2O_2 treatment, which was significantly inhibited by SP600125 and H89. Our results show for the first time the potential role of JNKs, p38-MAPK and MSK1 in the mechanism of transducing the oxidative stress-signal to HOX-1, possibly promoting cell survival and preserving homeostasis.

Keywords: Heme oxygenase-1; MSK1; JNKs; p38-MAPK; Oxidative stress

1. Introduction

Heme oxygenase (HOX) family members degrade heme to biliverdin, carbon monoxide (CO) and free iron in the mammalian cell [1]. HOX-1 is inducible while HOX-2 and -3 are constitutively expressed [2]. Ample evidence has demonstrated HOX-1 to be strongly stimulated by its substrate heme and multiple stress stimuli that increase the cellular production of reactive oxygen species (ROS) such as heat shock, hyperoxia, heavy metals and UV irradiation [3]. HOX products, CO and biliverdin, are of considerable physiological significance. In particular, CO is an important signalling gas that has been shown to play a prominent regulatory role for the tone of the cardiovascular system by promoting vasodilatation [4] and protecting hepatic microcirculation under stress conditions [5]. What is more, biliverdin, converted into bilirubin by biliverdin reductase, is a potent anti-oxidant [6]. In addition, being a regulator of iron homeostasis, HOX-1-mediated cytoprotection of cultured cells could be due to augmented cellular iron efflux [7].

As stated above, intracellular ROS levels are crucial to HOX-1 gene expression. Nevertheless, the precise mechanism, which modulates this response, is still unclear. ROS (i.e., the superoxide anion, hydrogen peroxide, the hydroxyl radical) are generated under a variety of physiological conditions and can interact with lipids, proteins and nucleotides. There is compelling evidence that through these interactions, increased

* Corresponding author. Tel.: +30 210 7274349; fax: +30 210 7274635.
E-mail address: ibeis@biol.uoa.gr (I. Beis).

0898-6568/$ - see front matter © 2006 Elsevier Inc. All rights reserved.
doi:10.1016/j.cellsig.2006.02.001

levels of ROS, have damaging effects and are involved in the pathogenesis of several diseases, including cardiac disorders such as arrhythmia, heart failure, hypercardia and ischemia/reperfusion (I/R) injury [8–10]. In support of this notion, recent studies have clearly shown that, being an adaptive enzyme to oxidative damage, HOX-1 gene expression levels are elevated in cases of coronary heart disease [11] and mitochondrial cardiomyopathy [12]. In addition, treatment with CO and biliverdin (byproducts of heme degradation) has been found to be effective in decreasing myocardial injury and improving cardiac function, offering protection against transplant-associated I/R heart graft injury [13].

Therefore, we undertook this study, in an effort to characterize the redox signalling intracellular pathways involved in H_2O_2-induced HOX-1 transcriptional regulation in the cardiomyocyte. To this end, H9c2 cardiomyoblasts were used as our experimental model, a clonal cell line derived from embryonic heart ventricle [14], which retains properties of signalling pathways of adult cardiomyocytes. In essence, under oxidative stress conditions, H9c2 myoblasts respond in a similar manner to myocytes in primary cultures or isolated heart experimental settings [15]. Thus, any finding in H9c2 cells also reflects the signalling transduction pathways activated in the complex and of diverse cell populations comprised, myocardium. This justifies the great number of reports using H9c2 myoblasts in order to investigate oxidative stress effects on the cardiomyocyte, a model, which has proven to be ideal for signal transduction studies [15–18].

A plethora of reports demonstrate that mitogen-activated protein kinases (MAPKs) play a crucial role in signal transduction of cellular stress stimuli as well as in regulation of cell proliferation and differentiation (reviewed in [19]). MAPKs constitute a widely distributed family of serine/threonine protein kinases that has been highly conserved through evolution and are activated through dual phosphorylation of a specific threonine and tyrosine residue by members of the MAPK kinases (MKKs) [20]. There are three best-characterized MAPK subfamilies: the extracellular signal-regulated kinases (ERKs), the cJun-N-terminal kinases (JNKs) and p38-MAPK [19,20]. Activated MAPKs are localized in both the cytoplasm and nucleus, where they interact with their substrates. In particular, they have been found to phosphorylate other protein kinases (i.e., $p90^{RSK}$, MAPKAPK2) as well as cytoskeletal proteins (i.e., tau) [21].

The downstream targets of MAPKs also include a number of transcription factors [19–21]. Hence, activated MAPKs can promote differential transcriptional stimulation of multiple genes via phosphorylation of members of, i.e., the MEF2 family, cJun, the ATF family and Elk [21]. Another MAPK substrate, recently identified, is the mitogen- and stress-activated protein kinase 1 (MSK1) [22]. This kinase is activated by ERKs or p38-MAPK and inhibited by the H89 compound [23,24]. Via its interaction with diverse transcription factors, MSK1 can also mediate transcriptional modulation leading to specific profiles of gene expression [22,25–27].

Nevertheless, there are controversial reports regarding the ultimate physiological outcome of these triggered responses, ranging from cell survival and adaptation (cardiac hypertrophy) to cell death (apoptosis). In an effort to assess the apparent important role that HOX-1 plays in heart physiology [11–13], particularly under stimulation by ROS [3], a major and crucial challenge in this field is to determine and characterize the signalling pathways involved in H_2O_2-induced HOX-1 expression pattern. In the present study, we demonstrate for the first time, the involvement of p38-MAPK/MSK1 and JNKs in HOX-1 mRNA upregulation in H_2O_2-treated cardiac cells. We also propose that the oxidative-stress signal can be potentially transduced to the nucleosome via the activator protein-1 (AP-1) components: ATF2 and cJun.

2. Materials and methods

2.1. Materials

Hydrogen peroxide was purchased from Merck (Darmstadt, Germany). DMSO, leupeptin, *trans*-epoxy-succinyl-L-leucylamido-(4-guanidino) butane (E-64), dithiothreitol (DTT), phenylmethylsulphonyl fluoride (PMSF), wortmannin and protein A-sepharose were obtained from Sigma-Aldrich (St. Louis, Missouri, USA). GF109230X, SP600125 and PD98059 were purchased from Calbiochem-Novabiochem (La Jolla, CA, USA), SB203580 and H89 were from Alexis Biochemicals (Lausen, Switzerland). [γ-^{32}P]ATP was from Hartmann Analytic GmbH (Braunschweig, Germany). Nitrocellulose (0.45 μm) was obtained from Schleicher and Schuell (Keene, NH, USA). Prestained molecular mass markers were from New England Biolabs (Beverly, MA, USA). Secondary antibodies were from DakoCytomation (Glostrup, Denmark). Primers for the detection of HOX-1 and GAPDH were synthesized by Invitrogen Life Technologies (California, USA). Super RX film was purchased from Fuji photo film GmbH (Dusseldorf, Germany). General laboratory reagents were purchased from Sigma-Aldrich or Merck.

2.2. Cell cultures and reagents

H9c2 cells (passage 18–25; American Type Culture Collection, Rockville, MD, USA) were cultured in DMEM (PAA Laboratories GmbH, Pasching, Austria) supplemented with 10% (v/v) heat inactivated fetal bovine serum (PAA Laboratories GmbH) and antibiotics, under an atmosphere of 95% air/5% CO_2 at 37 °C. Experiments were carried out using mononucleated myoblasts after serum had been withdrawn for 24 h. Hydrogen peroxide was added to the medium for the times and at the doses indicated. When pharmacological inhibitors were used, they were dissolved in DMSO and added to the medium 30 min prior to treatment with H_2O_2. Control experiments with DMSO alone were also performed for the same duration.

2.3. Protein extraction

Cells were extracted in buffer G [20 mM Tris–HCl pH 7.5, 20 mM *b*-glycerophosphate, 2 mM EDTA, 10 mM benzamidine, 20 mM NaF, 0.2 mM Na_3VO_4, 200 μM leupeptin, 10 μM E-64, 5 mM DTT, 300 μM PMSF and 0.5% (v/v) Triton X-100]. Samples were centrifuged (12,000 rpm, 5 min, 4 °C) and the supernatants boiled with 0.33 vol. of SDS-PAGE sample buffer [SB4X: 0.33 M Tris–HCl (pH 6.8), 10% (w/v) SDS, 13% (v/v) glycerol, 20% (v/v) 2-mercaptoethanol, 0.2% (w/v) bromophenol blue]. Protein concentrations were determined using the BioRad Bradford assay reagent (Bio-Rad, Hercules, California, USA).

2.4. Preparation of nuclear extracts

Nuclear extracts were prepared as previously described [28] with minor modifications. Cells were harvested into buffer A (10 mM Tris–HCl pH 7.9, 10 mM KCl, 1.5 mM $MgCl_2$, 0.3 mM Na_3VO_4, 200 μM leupeptin, 10 μM E-64, 5 mM DTT, 300 μM PMSF). Samples were centrifuged (10,000 rpm, 5 min, 4 °C)

and the supernatants discarded. Pellets were re-suspended in buffer A containing 0.1% (v/v) Nonidet P40 (10 min, 4 °C). After centrifugation (10,000 rpm, 5 min, 4 °C), pellets were re-suspended in buffer C [20 mM Hepes pH 7.9, 420 mM NaCl, 1.5 mM $MgCl_2$, 0.2 mM EDTA, 25% (v/v) glycerol, 0.3 mM Na_3VO_4, 200 μM leupeptin, 10 μM E-64, 5 mM DTT, 300 μM PMSF]. Protein concentrations were determined using the BioRad Bradford assay. For electrophoretic mobility shift assays (EMSAs), aliquots of nuclear extracts were stored at −80 °C. For immunoblotting analysis, nuclear extracts were boiled with 0.33 vol. of SB4X.

2.5. Immunoblotting

Proteins (30 μg) were separated by SDS-PAGE on 10% (w/v) polyacrylamide gels and transferred electrophoretically onto nitrocellulose membranes. Nonspecific binding sites were blocked with 5% (w/v) nonfat milk powder in TBST [20 mM Tris–HCl pH 7.5, 137 mM NaCl, 0.1% (v/v) Tween 20] for 30 min at room temperature. Subsequently, the membranes were incubated overnight with the appropriate primary antibody (1:1000) at 4 °C. Antibodies against total or phospho-ERKs, phospho-JNKs, phospho-p38-MAPK, phospho-MSK1, total or phospho-ATF2, total or phospho-cJun were from Cell Signaling Technology (Beverly, MA, USA), anti-actin was from Sigma-Aldrich (St. Louis, Missouri, USA), and anti-histone-1 was from Neomarkers (Fremont, USA). After washing in TBST (3 × 5 min), blots were incubated with the respective horseradish peroxidase-conjugated secondary antibody 1:5000 in TBST containing 1% (w/v) nonfat milk powder (60 min). After washing in TBST (3 × 5 min), bands were detected using enhanced chemiluminescense (ECL) (Amersham Biosciences, Uppsala, Sweden) and quantified by scanning densitometry (Gel Analyzer v. 1.0).

2.6. Immunoprecipitation

30 μl of protein A-sepharose [50% slurry in RBD buffer: 20 mM Tris–HCl pH 7.5, 1 mM EDTA, 1% (v/v) Triton X-100, 10% (v/v) glycerol, 100 mM KCl, 5 mM NaF, 0.2 mM Na_3VO_4, 5 mM $MgCl_2$, 0.05% (v/v) 2-mercaptoethanol] were incubated with 1 μl of phospho-ATF2 or phospho-cJun antibody on a rotating wheel (4 °C, O/N). After a brief spin (10,000 rpm, 1 min, 4 °C), the formed complexes were washed in RBD buffer (×3). Untreated (control) or H_2O_2-treated cells were scraped into RBD buffer containing 200 μM leupeptin, 10 μM E-64, 5 mM DTT and 300 μM PMSF. Samples were extracted on ice (10 min) and centrifuged (10,000 rpm, 5 min, 4 °C). An aliquot of the supernatants was boiled with 0.33 vol. of SB4X, while the rest was incubated with the protein A-sepharose/antibody complexes (4 h, 4 °C). After centrifugation (10,000 rpm, 1 min, 4 °C), the supernatants (S/N) were boiled with 0.33 vol. of SB4X. Pellets were washed (×3) with RBD buffer and finally re-suspended (immunoprecipitate-IP) and boiled in 40 μl of (SB2X).

2.7. RNA preparation, cDNA synthesis and ratiometric reverse transcription PCR (RT-PCR)

The expression of endogenous HOX-1 was determined by ratiometric reverse transcription of total RNA followed by PCR analysis. Total RNA was extracted from cells using Trizol (Invitrogen Life Technologies), according to the manufacturer's instructions. For cDNA synthesis, 2 μg of total RNA was denatured in the presence of 5 pmol oligo-dT primer in a reaction volume of 13.5 μl at 65 °C for 5 min. Reverse transcription was performed with M-MLV Reverse Transcriptase (Invitrogen Life Technologies), first strand buffer (Promega, Madison, USA), dithiothreitol (Promega) and deoxy-nucleotide triphosphates (dNTPs) (Promega). The first strand reaction was incubated at 37 °C for 1 h. Termination of the reaction was achieved by inactivation of the reverse transcriptase at 70 °C for 5 min. PCR for HOX-1 was performed using 1.5 Units Taq (Bioron GmbH, Ludwigshafen, Germany) with sense 5′-GAG AAT TCT GAG TTC ATG AGG-3′ and antisense 5′-TGC GAG CAC GAT AGA GCT G-3′ primers, based on the sequence of rat HOX-1 (Genbank accession no. AI179610). These primers amplify a 472-base pair PCR product. After a 5-s denaturation at 94 °C, PCR was carried out for 28 cycles (94 °C for 30 s, 59 °C for 30 s and 72 °C for 30 s), and then a final extension was done at 72 °C for 4 min. PCR (25 cycles) for GAPDH was performed using the following primers: sense 5′-ACC ACA GTC CAT GCC ATC AC-3′ and antisense 5′-TCC ACC ACC CTG TTG CTG TA-3′ (Genbank accession no. X02231). cDNA samples derived from "control" and treated cells were always amplified simultaneously. PCR products were separated on a 2% (w/v) agarose gel supplemented with ethidium bromide (EtBr) at a final concentration of 100 μg/l. Band intensities were determined using an appropriate image analysis programme (Gel Analyzer v. 1.0). All values were normalized for the amount of GAPDH mRNA and estimation of fragment band size (HOX-1 472 bp, GAPDH 452 bp) was performed by comparison with GeneRuler 100-bp DNA ladder (Fermentas Life Sciences Inc., Hanover, USA).

2.8. Electrophoretic mobility shift assay

The oligonucleotide containing consensus AP-1 sequence was from Promega. 3.5 pmol of cAP-1 was 5′ end-labelled with [γ-^{32}P]ATP by incubating for 30 min at 37 °C along with T4 polynucleotide kinase buffer 10× (Promega), 10 Units of T4 polynucleotide kinase (Promega) and 15 μCi [γ-^{32}P]ATP. After the reaction was terminated by the addition of EDTA (15 μM), unincorporated [γ-^{32}P]ATP was removed using a Sephadex G50 column in TE buffer (10 mM Tris–HCl pH 8.0, 1 mM EDTA). Nuclear extracts (10 μg) were incubated (10 min, RT) in binding buffer (50 mM Tris–HCl pH 7.5, 250 mM NaCl, 5 mM EDTA, 25% (v/v) glycerol, 1 mM DTT, 1 μg poly dI–dC) in a final volume of 20 μl. Subsequently, 0.5 ng of radiolabeled oligonucleotide was added (20 min, RT). DNA–protein complexes were resolved on a 5% (w/v) non-denaturing polyacrylamide gel (120 V, 1 h). Gels were dried and exposed to Super RX photo film for 24 h. For competition experiments, unlabeled cAP-1 oligonucleotide (4–40 ng) was added prior to the addition of radiolabelled cAP-1.

2.9. Statistical evaluations

All data are presented as means ± S.E.M. Comparisons between control and treatment were performed using Student's paired *t*-test. A value of at least $P < 0.05$ was considered to be statistically significant.

3. Results

3.1. H_2O_2 stimulates HOX-1 mRNA levels in H9c2 cells. Involvement of p38-MAPK, JNKs and MSK1

There is emerging evidence revealing HOX-1 diverse biological and cytoprotective effects against oxidative damage in the myocardial tissue. Accumulating studies provide new insights into the knowledge of the mechanism regulating HOX-1 response to oxidative stress, in the form of H_2O_2 [11–13]. In order to investigate the mechanism regulating HOX-1 transcriptional upregulation under oxidative stress conditions, H9c2 cells were treated with 200 μM H_2O_2, a concentration used routinely for gene expression studies in cardiomyocyte experimental settings exposed to oxidative stress [29]. Thus, HOX-1 mRNA was found to be induced from 2 h (3.7 ± 0.87-fold relative to control), maximized at 6 h (6.3 ± 0.3-fold relative to control) (Fig. 1A, upper panel, and C) and remaining elevated for 24 h (3.88 ± 0.07-fold relative to control). Subsequently, to probe into the actual pathways transducing this response, we tried to determine the signalling cascades involved in the H_2O_2-stimulated HOX-1 transcript levels. To this end, various pharmacological inhibitors were used: SB203580 (10 μM): a p38-MAPK inhibitor, PD98059 (25 μM): that blocks the ERK1/2 pathway, SP600125 (10 μM): a JNKs inhibitor, H89 (10 μM): a selective inhibitor of MSK1 as well as catalase (75 U/ml), which decomposes

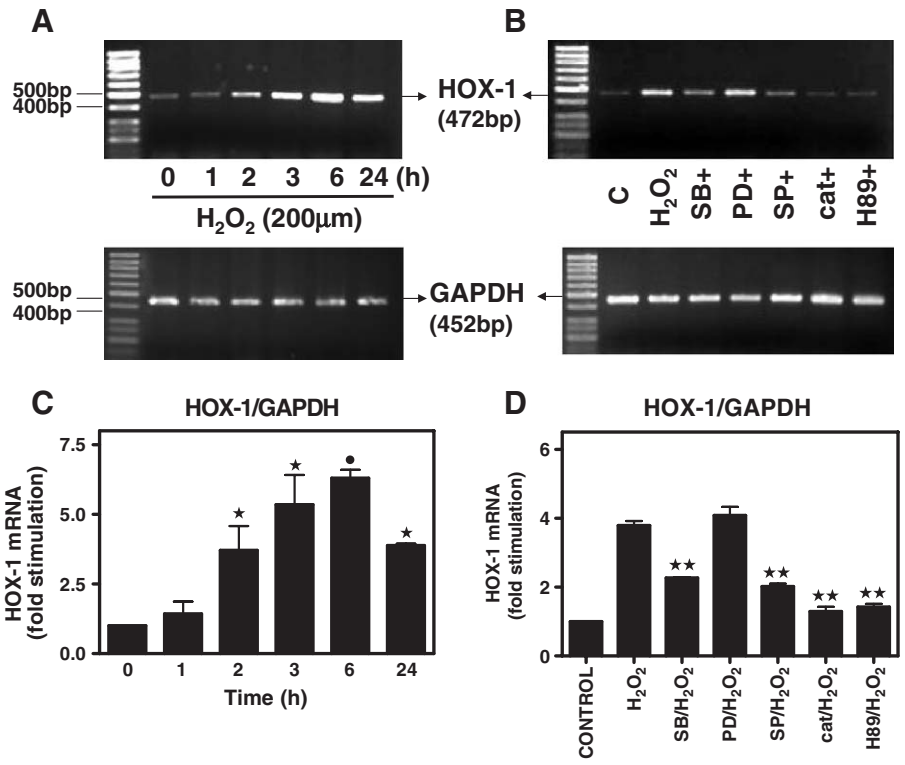

Fig. 1. Kinetics of H_2O_2-induced HOX-1 mRNA upregulation in H9c2 cardiomyoblasts: a p38-MAPK, JNKs and MSK1-mediated response. (A) H9c2 cells were exposed to 200 μM H_2O_2 for the times indicated. (B) H9c2 cells were left untreated (C: control) or pre-incubated with 10 μM SB203580, 25 μM PD98059, 10 μM SP600125, 75 (U/ml) catalase and 10 μM H89 for 30 min, then exposed to 200 μM H_2O_2 for 3 h in the absence or presence of the inhibitors. RNA was extracted and expression of HOX-1 (A and B upper panels) as well as GAPDH (A and B lower panels) mRNA was analyzed by ratiometric RT-PCR. The positions of the 500- and 400-bp markers are indicated on the left of the panels. After densitometric analysis of the PCR products, results were normalized for GAPDH and the data is presented (C and D) as fold stimulation. Results are means ± S.E.M. for at least three independent experiments. *$p<0.01$, •$p<0.001$ compared to control values. **$p<0.01$ compared to identically treated cells in the absence of inhibitors.

H_2O_2. Cells were left untreated (control-C) or were incubated with (a) either DMSO or (b) the inhibitors alone or (c) with the inhibitors followed by exposure to 200 μM H_2O_2 for 3 h. DMSO as well as the inhibitors alone had no effect on HOX-1 mRNA levels (data not shown). As shown in Fig. 1B (upper panel) and D, we observed that pre-treatment of H9c2 cells with SB203580 and SP600125 markedly reduced H_2O_2-stimulated HOX-1 response, by 40 ± 5% and 47 ± 5%, respectively. Furthermore, the latter was abolished in the presence of H89, while PD98059 failed to change the observed response. These results indicate that p38-MAPK, JNKs and MSK1 participate in H_2O_2-induced HOX-1 mRNA upregulation in H9c2 cells. In contrast, ERKs do not seem to have any contribution. What is more, the observed effect was shown to be attributed to the exogenously added H_2O_2 since it was completely inhibited in the presence of catalase (Fig. 1B, upper panel, and D).

3.2. All three MAPK subfamilies are activated in H_2O_2-treated H9c2 cells

In light of the ratiometric RT-PCR results, implicating p38-MAPK and JNKs in HOX-1 mRNA stimulation by H_2O_2, we attempted to further investigate the time- and dose-dependent activation profile of these MAPKs by Western blotting. As shown in Fig. 2A and C, a rapid onset of p38-MAPK phosphorylation was observed at 5 min (4.3 ± 0.8-fold relative to control) with maximal values being attained at 15–30 min (4.8 ± 0.6-fold relative to control), declining thereafter. A slightly more delayed but equally significant response of both p46 (4.5 ± 0.5-fold relative to control) and p54 (6.5 ± 1.7 compared to control) JNKs was detected at 15 min of H_2O_2 treatment (Fig. 2B,D). Interestingly, immunoblotting of phosphorylated p42 and p44 ERKs revealed their activation, which was maximal at 15 min (3.7 ± 0.4- and 5 ± 0.5-fold relative to

Fig. 2. Time- and dose-dependent phosphorylation profile of p38-MAPK, JNK1/2 and ERK1/2 by H_2O_2 in H9c2 cardiomyoblasts. H9c2 cells were left untreated (C: control) or were exposed to 200 μM H_2O_2 for the times indicated (A) or to various H_2O_2 concentrations for 15 min (B). Cell extracts (30 μg) were subjected to SDS-PAGE and immunoblotted with antibodies for phosphorylated: p38-MAPK (Thr180/Tyr182) (A and B upper panel), JNK1/2 (Thr183/Tyr185) (A and B second panel from top) and ERK1/2 (Thr202/Tyr204) (A and B third panel from top) as well as for total levels of ERK1/2 (A and B bottom panel). Phospho-p38-MAPK (C and F), phospho-JNK1/2 (D and G) and phospho-ERK1/2 (E and H) were quantified by laser scanning densitometry. Blots and results shown are representative of at least three independent experiments. Results are means ± S.E.M. for at least three independent experiments. **$p<0.05$, *$p<0.01$, •$p<0.001$ compared to control values.

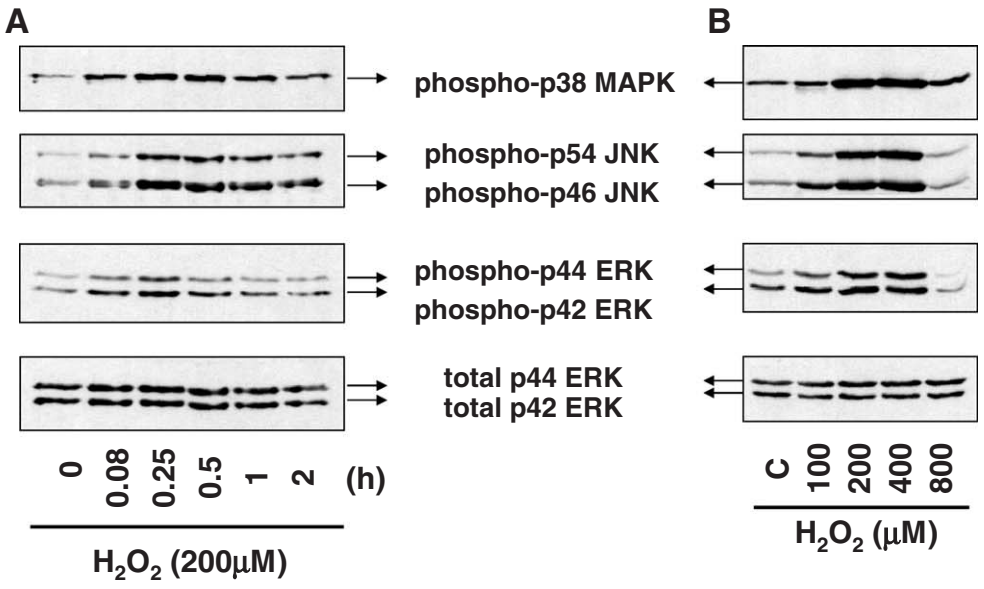
A
B
phospho-p38 MAPK
phospho-p54 JNK
phospho-p46 JNK
phospho-p44 ERK
phospho-p42 ERK
total p44 ERK
total p42 ERK
0 0.08 0.25 0.5 1 2 (h)
H2O2 (200μM)
C 100 200 400 800
H2O2 (μM)

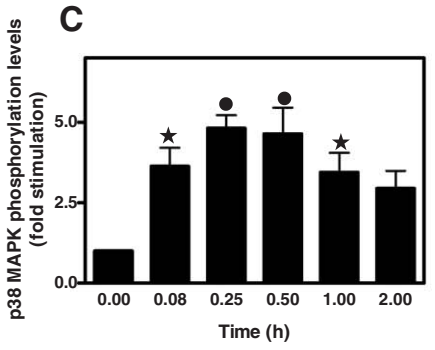
C
p38 MAPK phosphorylation levels (fold stimulation)
0.0 2.5 5.0
0.00 0.08 0.25 0.50 1.00 2.00
Time (h)

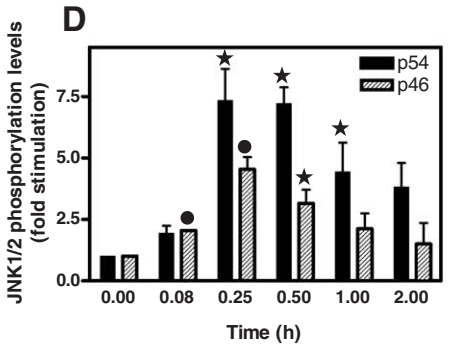
D
JNK1/2 phosphorylation levels (fold stimulation)
p54
p46
0.0 2.5 5.0 7.5
0.00 0.08 0.25 0.50 1.00 2.00
Time (h)

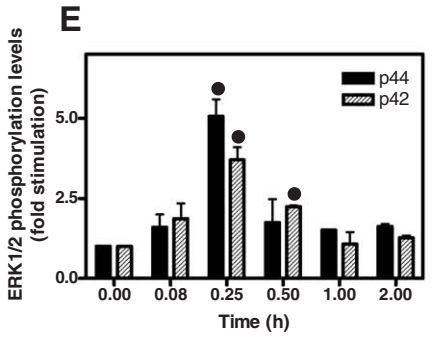
E
ERK1/2 phosphorylation levels (fold stimulation)
p44
p42
0.0 2.5 5.0
0.00 0.08 0.25 0.50 1.00 2.00
Time (h)

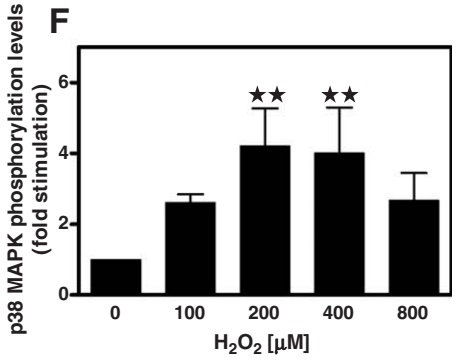
F
p38 MAPK phosphorylation levels (fold stimulation)
0 2 4 6
0 100 200 400 800
H2O2 [μM]

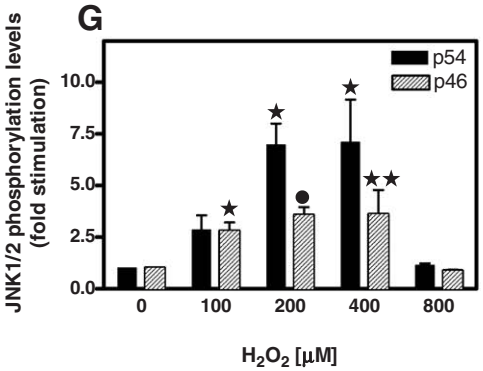
G
JNK1/2 phosphorylation levels (fold stimulation)
p54
p46
0.0 2.5 5.0 7.5 10.0
0 100 200 400 800
H2O2 [μM]

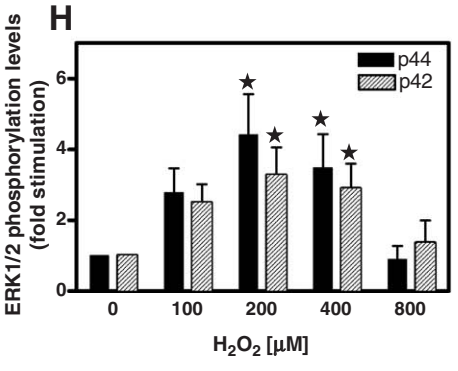
H
ERK1/2 phosphorylation levels (fold stimulation)
p44
p42
0 2 4 6
0 100 200 400 800
H2O2 [μM]

control, respectively). Total levels of all three subfamilies did not change during these interventions (data shown only for total ERKs—Fig. 2A,B, bottom panels). The specificity of H_2O_2-dependent induction of the MAPKs phosphorylation was confirmed by dose-dependent experiments. The minimum concentration that reproducibly induced all three MAPK-subfamilies activation after 15 min of treatment was identified at 200 μM (Fig. 2B, F, G and H).

3.3. Activation of MSK1 by H_2O_2 in H9c2 cells

We also analyzed and evaluated MSK1 involvement in HOX-1 stimulation by H_2O_2, by examining MSK1 phosphorylation profile (Fig. 3A,C). Cell extracts were immunoblotted with an antibody that specifically recognizes MSK1 when phosphorylated at Thr581. Maximal levels of the kinase phosphorylation were attained 15 min (7.8 ± 0.3-fold relative to control) after the onset of stimulation, declining to basal levels after 60 min. Furthermore, using various inhibitors, the contribution of a number of signalling pathways to MSK1 phosphorylation was assessed. Our results suggest that the latter is mediated via p38-MAPK, since SB203580 completely ablated it (Fig. 3B,D). Inhibitors of JNKs and ERKs had no effect. This was also the case with H89, which has previously been shown to affect directly the activity of MSK1 without reducing its phosphorylation levels [30]. Equal protein loading was verified by reprobing the membranes with an anti-actin antibody (Fig. 3A,B, bottom panels).

3.4. ATF2 and cJun are both downstream targets of MSK1 in H_2O_2-treated H9c2 cells

To our knowledge, this is the first report of MSK1 activation by H_2O_2 in cardiac cells. Therefore, the detection of possible MSK1 targets potentially transducing the oxidative stress signal to HOX-1 gene appeared exquisitely interesting. Monitoring the time profile of both ATF2 (Fig. 4A,C) and cJun (Fig. 5A,C) phosphorylation in H9c2 cells treated with H_2O_2, we observed that their maximal activation was delayed compared to that of MSK1, being reached at 30 min (4.1 ± 0.2-fold relative to control) and 60 min (6.9 ± 0.6-fold relative to control), respectively. This prompted us to emphasize on the probable role of MSK1 in the observed response of the two transcription factors of interest. Our results showed that H89 as well as SP600125, completely inhibited ATF2 and cJun phosphorylation by H_2O_2, while no SB203580 nor PD98059 had any effect, discarding the involvement of p38-MAPK or ERKs in this response (Figs. 4B, D and 5B,D).

Equal protein loading of nuclear extracts for these experiments was confirmed by blotting with an antibody against histone 1 (Fig. 4A,B), total ATF2 (Fig. 4A, middle panel) and total cJun levels (Fig. 5A,B, lower panels). In correlation to other group's findings [28,31], we observed that the antibody

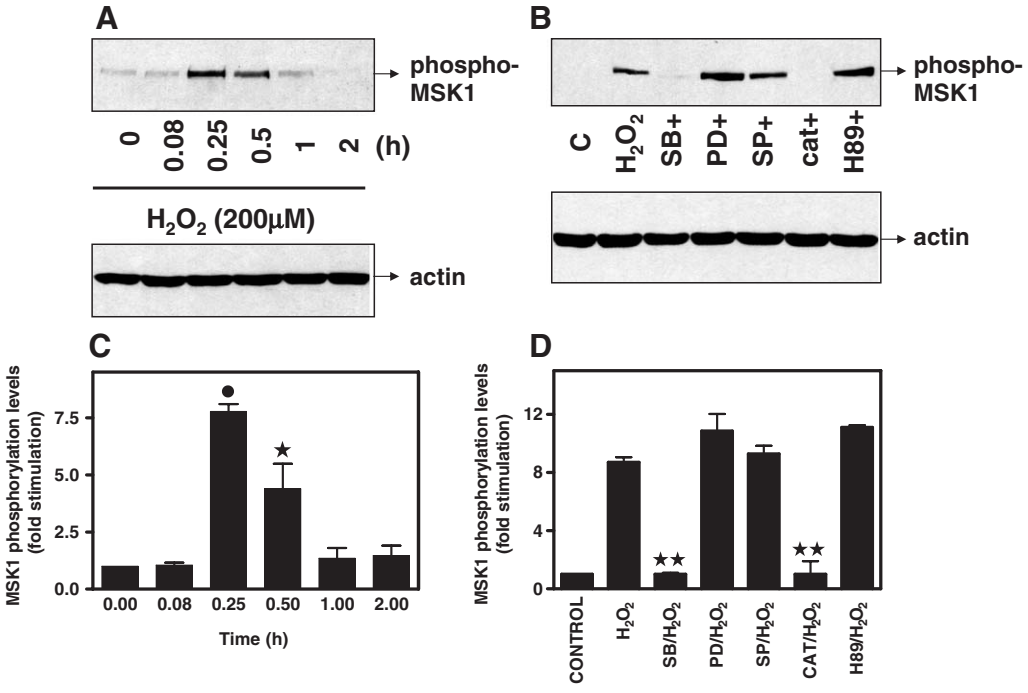

Fig. 3. (A) Time course of H_2O_2-induced MSK1 phosphorylation in H9c2 cardiomyoblasts. H9c2 cells were left untreated (C: control) or were exposed to 200 μM H_2O_2 for the times indicated. (B) Effect of SB203580, PD98059, SP600125, catalase and H89 on MSK1 response. H9c2 cells were untreated or pre-incubated with 10 μM SB203580, 25 μM PD98059, 10 μM SP600125, 75 (U/ml) catalase and 10 μM H89 for 30 min, then exposed to 200 μM H_2O_2 for 15 min in the absence or presence of the inhibitors. Cell extracts (30 μg) were subjected to SDS-PAGE and immunoblotted with antibody for phosphorylated MSK1 (Thr581) (A and B upper panels). To verify equal loading, the membranes were then stripped and re-incubated with anti-actin antibody (A and B lower panels). Bands were quantified by laser scanning densitometry (C and D). Blots and results shown are representative of at least three independent experiments. Results are means ± S.E.M. for at least three independent experiments. *$p < 0.01$, •$p < 0.001$ compared to control values. **$p < 0.001$ compared to identically treated cells in the absence of inhibitors.

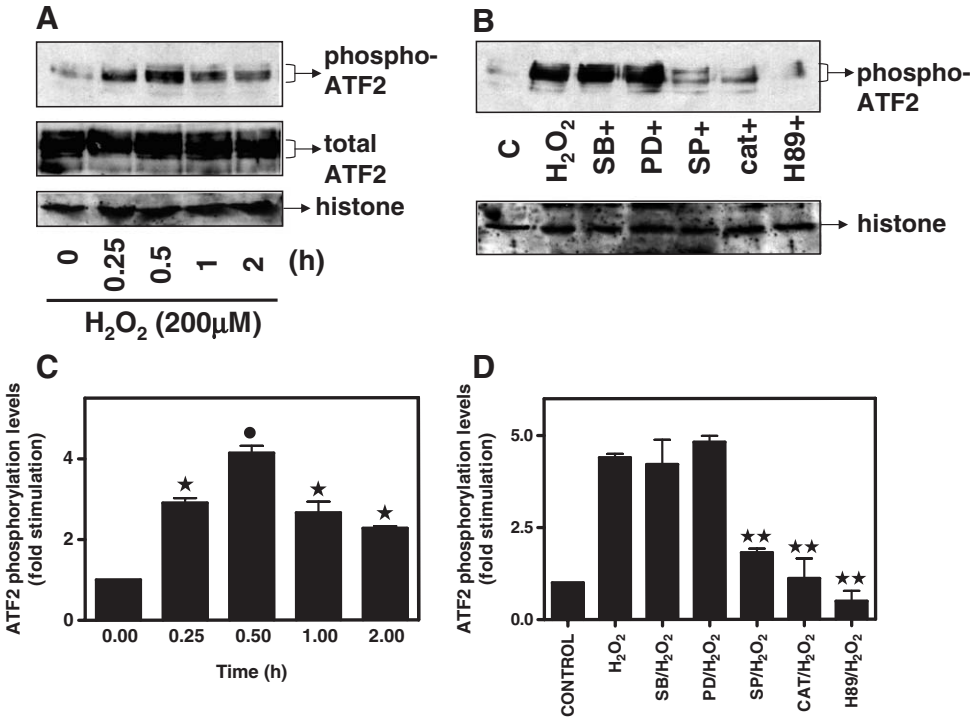

Fig. 4. (A) Time course of H_2O_2-induced ATF2 phosphorylation in H9c2 cardiomyoblasts. H9c2 cells were exposed to 200 μM H_2O_2 for the times indicated. (B) Effect of SB203580, PD98059, SP600125, catalase and H89 on ATF2 response. H9c2 cells were left untreated (C: control) or were pre-incubated with 10 μM SB203580, 25 μM PD98059, 10 μM SP600125, 75 (U/ml) catalase and 10 μM H89 for 30 min, then exposed to 200 μM H_2O_2 for 30 min in the absence or presence of the inhibitors. Nuclear extracts (30 μg) were subjected to SDS-PAGE and immunoblotted with an antibody for phosphorylated ATF2 (Thr71) (A and B upper panels). To verify equal loading, the membranes were then stripped and re-incubated with anti-histone antibody (A and B lower panels). Total levels of ATF2 were also detected (A middle panel). Bands were quantified by laser scanning densitometry (C and D). Blots and results shown are representative of at least three independent experiments. Results are means ± S.E.M. for at least three independent experiments. *$p<0.05$, •$p<0.001$ compared to control values. **$p<0.001$ compared to identically treated cells in the absence of inhibitors.

specific for the phosphorylated as well as total levels of ATF2 detects two bands at approximately 70 kDa, both of which exhibit a parallel response pattern (Fig. 4A,B). Moreover, the anti-phosphorylated cJun antibody detects a single band in untreated cells at ~46 kDa and a second one of reduced mobility in treated cells, possibly representing an even more highly phosphorylated form. In addition to this, the antibody against total cJun levels is also found to detect a second band of reduced mobility in treated cells, indicative of the phosphorylated form of the transcription factor [28,31].

To further substantiate MSK1 interaction with ATF2 and cJun, we made an effort to determine whether MSK1 could be co-immunoprecipitated with either transcription factor. For this purpose, anti-phospho-ATF2 was used as the primary antibody in the immunoprecipitation of cell lysates from H9c2 cells left untreated or exposed to H_2O_2 for 30 min (Fig. 6A). The specific anti-phospho-MSK1 antibody was then used to test whether phospho-ATF2 could pull down phosphorylated MSK1. As shown in Fig. 6A and B, phosphorylation of MSK1 was detected in the immunoprecipitate of H_2O_2-exposed cells' lysate, previously incubated with anti-phospho-ATF2 or, alternatively, anti-phospho-cJun antibody. These findings imply that signalling complexes comprised of phospho-MSK1 and phoshpo-ATF2 or phospho-cJun can be formed under these conditions. In Fig. 6C, the immunodepletion of phospho-ATF2, after the addition of the respective antibody, is shown.

3.5. H_2O_2 stimulates AP1 DNA binding activity

Using EMSA, we next tried to delineate the possible role of AP1 elements in transducing the signal downstream from ATF2 and cJun. Both transcription factors have been previously found to bind to AP1 elements [32]. In accordance with our hypothesis, H_2O_2-induced activation of ATF2 and cJun were concordant with an increase in AP1 binding activity. In particular, the latter exhibited a similar time-dependent profile increasing from 30 min (1.75 ± 0.09-fold relative to control) and attaining maximal values at 1 h (3.57 ± 0.19-fold relative to control), while some basal binding was also observed in the absence of stimulation (Fig. 7A,B). What is more, pre-incubation of H9c2 cells with SP600125 or H89, was found to partially inhibit the H_2O_2-induced AP-1 binding activity, implicating JNKs as well as MSK1 in the signalling cascade leading to this induction (Fig. 7C,D). In the presence of 10-fold excess of non-radiolabeled AP-1 oligonucleotide, the detected H_2O_2-induced band of the autoradiograph was diminished (data not shown) confirming that it represents an AP-1 binding complex.

4. Discussion

Exerting a cytoprotective effect against oxidative injury, HOX-1 has been identified as a critical enzyme preserving

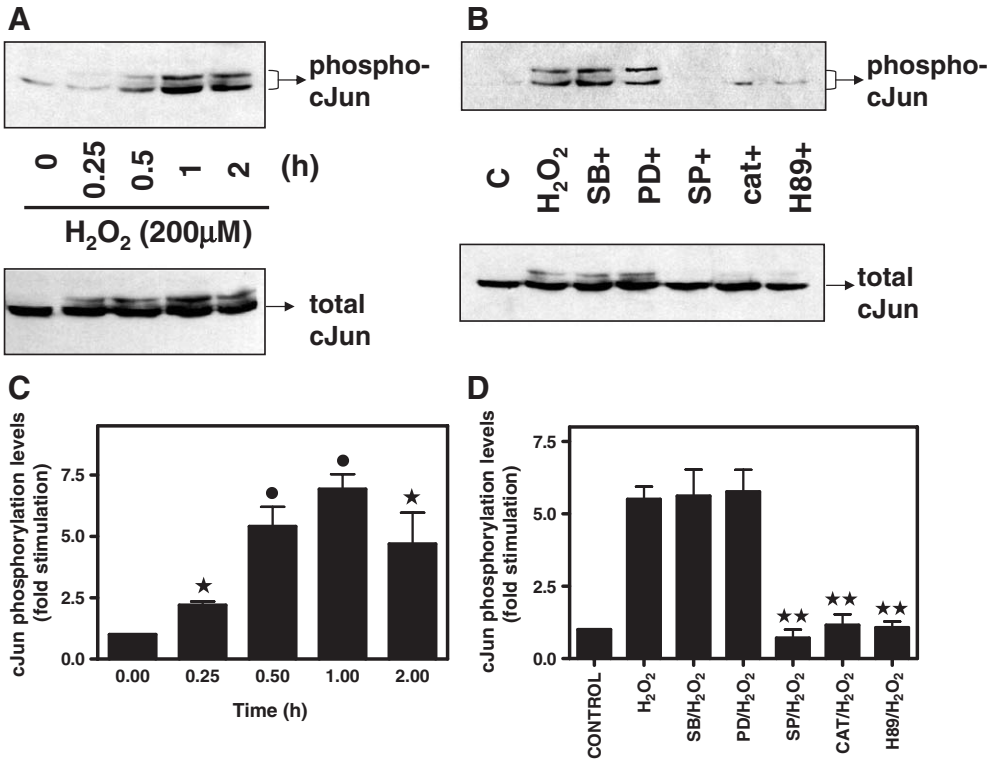

Fig. 5. (A) Time course of H_2O_2-induced cJun phosphorylation in H9c2 cardiomyoblasts. H9c2 cells were exposed to 200 μM H_2O_2 for the times indicated. (B) Effect of SB203580, PD98059, SP600125, catalase and H89 on cJun response. H9c2 cells were left untreated (C: control) or pre-incubated with 10 μM SB203580, 25 μM PD98059, 10 μM SP600125, 75 (U/ml) catalase and 10 μM H89 for 30 min, then exposed to 200 μM H_2O_2 for 60 min in the absence or presence of the inhibitors. Nuclear extracts (30 μg) were subjected to SDS-PAGE and immunoblotted with an antibody for phosphorylated cJun (Ser63) (A and B upper panels). To verify equal loading, the membranes were then stripped and re-incubated with an antibody against the total levels of cJun (A and B lower panels). Bands were quantified by laser scanning densitometry (C and D). Blots and results shown are representative of at least three independent experiments. Results are means ± S.E.M. for at least three independent experiments. *$p<0.05$, •$p<0.001$ compared to control values. **$p<0.05$ compared to identically treated cells in the absence of inhibitors.

cellular homeostasis [33] in both cultured cell systems, as well as in in vivo studies [34]. Accumulating recent reports, account for a key role of HOX-1 system in physiology and disease, via the activity of heme degradation products. These data support HOX-1 as a considerably sensitive inducible protein in response to stressful stimuli, regulating numerous cellular functions

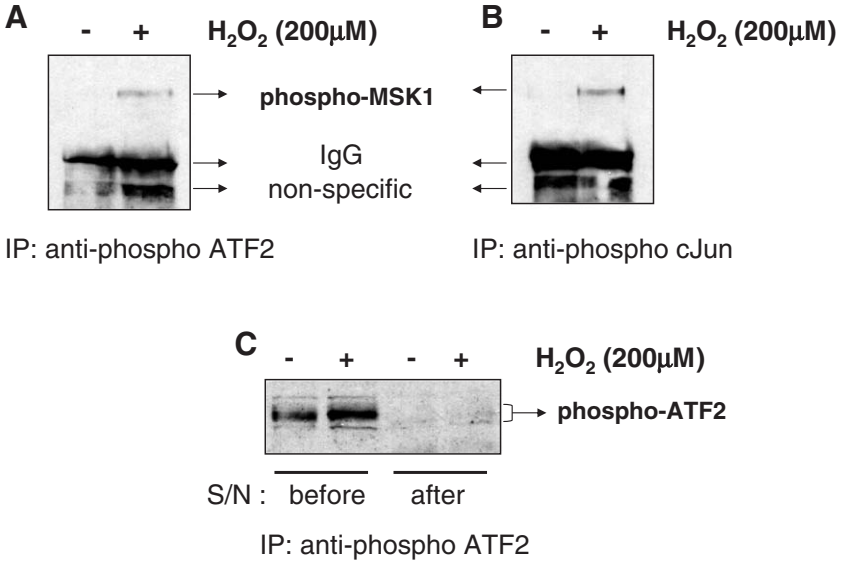

Fig. 6. Potential signalling complexes comprised of MSK1 and ATF2 (A) or cJun (B). H9c2 cells were left untreated or exposed to 200 μM H_2O_2 for 30 min as indicated. Equal amounts of cell lysates were subjected to immunoprecipitation (IP) with specific antibodies against phospho-ATF2 (A) or phospho-c Jun (B). The immunoprecipitates were subsequently blotted with the phospho-MSK1 specific antibody (A, B). (C) Supernatants (S/N) from untreated or H_2O_2-treated cells were also blotted for phospho-ATF2 before and after the addition of the antibody, in order to verify the immunodepletion of the latter.

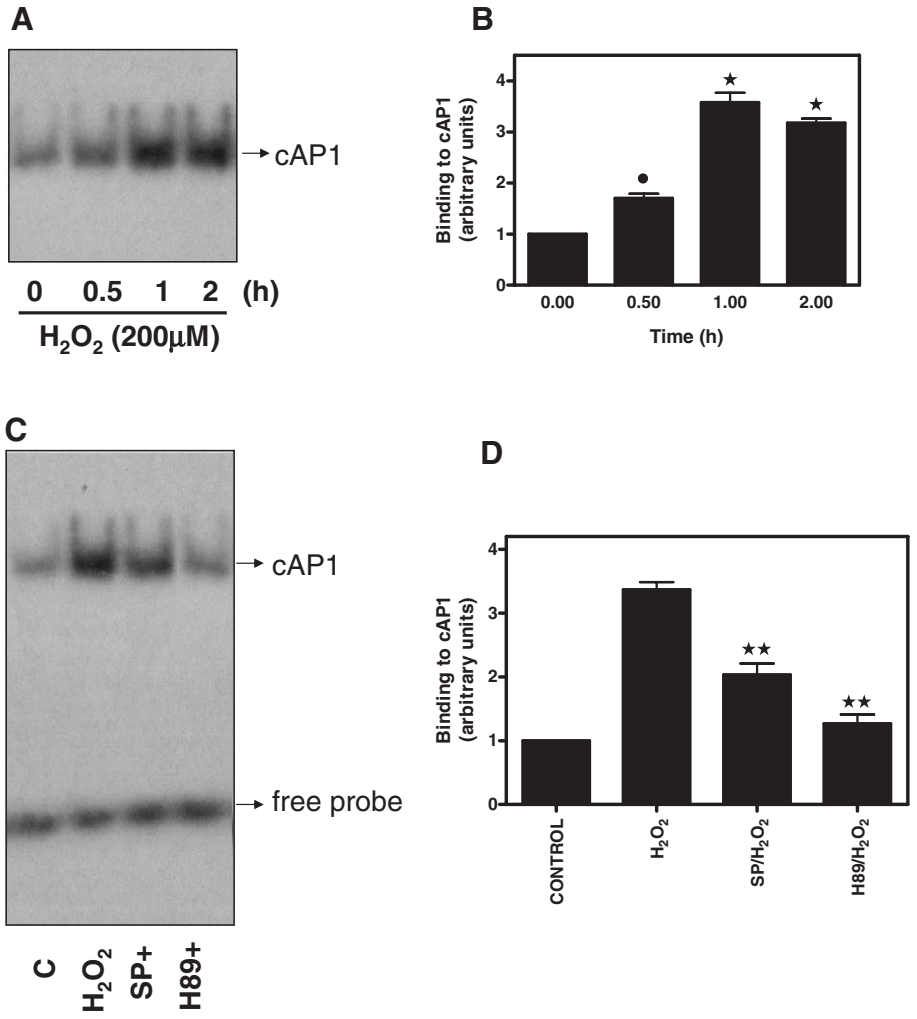

Fig. 7. Transcription factor binding to a cAP-1 sequence increases in response to H_2O_2 stimulation. (A) H9c2 cells were exposed to 200 μM H_2O_2 for the times indicated. Nuclear extracts were analyzed by EMSA using a radiolabeled oligonucleotide containing a cAP1 sequence. (C) JNKs and MSK1 potentially contribute to H_2O_2-stimulated AP-1 binding activity. H9c2 cells were left untreated (C: control) or pre-incubated with 10 μM SP600125 and 10 μM H89 for 30 min, then exposed to 200 μM H_2O_2 for 1 h, in the absence or presence of the inhibitors. Nuclear extracts were analyzed by EMSA. Representative autoradiographs are presented from at least three independent experiments with similar results. (B, D) Densitometric analysis of autoradiographs represented in panels A and C, respectively. Results are means ± S.E.M. for at least three independent experiments. $^{\bullet}p<0.05$, $^{*}p<0.001$ compared to control values. $^{**}p<0.01$ compared to identically treated cells in the absence of inhibitors. The free probe can be seen at the bottom of the autoradiograph in panel C.

ranging from signal transduction to anti-oxidant, anti-apoptotic and vascular activities (reviewed in Ref. [35]). Evidently, it is of high importance to elucidate the signalling cascades involved in HOX-1 regulation, particularly in the cardiac myocyte, with ROS being known to have deleterious effects on vasculature and the myocardium.

Therefore, we tried to determine the signalling cascades involved in H_2O_2-induced HOX-1 mRNA upregulation in H9c2 cells, since the mechanism regulating the expression of this pivotal gene, under oxidative stress conditions, remains elusive. Noticeably, in respect to the signalling pathways mediating HOX-1 transcriptional regulation, numerous studies have reported the involvement of p38-MAPK in the latter by a plethora of stimuli including statins [36], NAD(P)H oxidase inhibitors [37], TGFβ [38] and hypoxia [39]. On the other hand, fewer investigators have observed the participation of JNKs in HOX-1 mRNA levels stimulation. In particular, Oguro et al. [40] and Zhang et al. [41] have pointed to the critical intermediacy of JNKs, in HOX-1 gene transcriptional regulation, after treatment with the glutathione depletor phorone [40] or ischemia/reperfusion [41], respectively. In addition, ERK pathway has been found to mediate HOX-1 gene expression induced by NO [42] and ischemia/reperfusion [41]. We have shown that HOX-1 gene transcription is induced in H9c2 cells exposed to oxidative stress [H_2O_2] (Fig. 1A), via activation of multiple signalling pathways including: p38-MAPK, JNKs and MSK1 (Fig. 1B). On the contrary, PD98059 did not block H_2O_2-induced HOX-1 mRNA stimulation in our experimental setting. Collectively, it becomes evident that the involvement of MAPKs in the transcriptional regulation of HOX-1 depends on the nature of the stimulus applied.

Keyse and Tyrrell were the first to show the accumulation of HOX-1 mRNA after treatment of human skin fibroblasts with 100 μM H_2O_2 [43]. Furthermore, using a microarray approach, Kemp et al. have found that HOX-1 mRNA levels were substantially upregulated after 2 h as well as after 4 h of H_2O_2

treatment (200 μM) in neonatal rat ventricular cardiac myocytes [29].

MAPKs activation under oxidative stress is well established in cardiac myocytes [44]. Intriguingly, in our hands, although all three subfamilies were found to be phosphorylated by 200 μM H_2O_2 in H9c2 cells (Fig. 2), only p38-MAPK and JNKs mediated HOX-1 mRNA upregulation (Fig. 1B). This result could be justified in the context of p38-MAPK and JNKs being the two principal MAPK subfamilies mediating cellular stress signals, whereas ERKs are primarily associated with cell growth and proliferation [21]. In correlation to our findings, in a study by Turner et al. in H9c2 cells, all three MAPK subfamilies were also shown to be phosphorylated in the range of 200–400 μM after exposure to H_2O_2 [16].

Among MAPKs substrates are members of the MSKs: serine/threonine protein kinases, which are activated by ERKs and p38-MAPK [22,45]. As shown in Fig. 1B, H89, a selective MSK1 inhibitor [23,25,46], markedly blocked HOX-1 mRNA upregulation by H_2O_2. In correlation to MSK1's detected involvement in HOX-1 transcriptional regulation, the time course of MSK1 phosphorylation at Thr581 was found to closely follow that of p38-MAPK, attaining its maximal values after 15 min of H_2O_2 treatment (Fig. 3A). To our knowledge, our study represents the first to demonstrate not only MSK1 phosphorylation under oxidative stress conditions in the cardiac myocyte, but also the kinase role in H_2O_2-induced HOX-1 gene expression.

Pharmacological inhibitors of PKC (GF109203X-10 μM) or PI3K (wortmannin-100 nM) failed to attenuate MSK1 phosphorylation (data not shown). On the other hand, SB203580 diminished the latter, implicating p38-MAPK in this response (Fig. 3B, lane 3). No involvement of ERKs in MSK1 phosphorylation was detected (Fig. 3B, lane 4). This result is in accordance with a study by Weber et al., in sections from hippocampal or cortical tissue from Alzheimer's (AD) disease patients, with oxidative stress characteristics known to precede the classical pathological hallmarks of AD [47]. Indeed, they reported co-localization of phospho-MSK1 (Thr581) with activated p38-MAPK and phospho-MSK1 (Ser376) with activated ERK, suggesting preferential phosphorylation sites for the two upstream effectors.

So far, numerous studies have pointed to MSK1 activation downstream of p38-MAPK by a great variety of stimuli so diverse as: platelet-derived growth factor (PDGF) in peritubular smooth muscle cells (PSMC) [48], forskolin in NIH3T3 cells [26], *N*-methyl-D-aspartate (NMDA) in cortical neurons [45], tumour necrosis factor in endothelial cells [27] and ultraviolet B irradiation in mouse epidermal JB6 cells [49]. These findings, along with our results, mark the prominent role of MSK1 as a convergent point, mediating the transduction of extracellular or intracellular signals to downstream effectors, thus contributing to cell homeostasis and equilibrium preservation.

Several studies have identified mainly transcription factors (CREB [26,27,50], ATF1 [51], NfKB [25]), as well as STAT3 (signal transducer and activator of transcription 3) [46], 4E-BP1 (eIF4E-binding protein 1) [52] and histone H3/HMG-14 [23], as indirect or direct targets of MSK1. All of the above provide evidence of the latter being a link completing the circuit between cell surface and the nucleosome. In an effort to assess potential substrates of MSK1 in H_2O_2-treated H9c2 cells, and considering that ATF2 and cJun transcription factors have been previously shown to mediate oxidative stress effects in gene expression in the cardiac myocyte [53], we first analyzed ATF2 (Fig. 4A) and cJun (Fig. 5A) time-dependent phosphorylation patterns. In particular, ATF2 phosphorylation was found to be maximal (30 min) earlier than that of cJun (60 min), with both responses completely abrogated by SP600125 and H89 (Figs. 4B and 5B, respectively). Hence, JNKs and MSK1 seem to mediate ATF2 (Thr71) and cJun (Ser63) phosphorylation, unlike ERK and p38-MAPK pathway that have no apparent participation. Thus, the diverse interactions promoted under these interventions modulate analogously the cellular transcriptional response.

This result correlated well with previous reports of cJun and ATF2, JNK-dependent phosphorylation [54]. Interestingly, while SB203580 completely abrogated H_2O_2-induced MSK1 phosphorylation at Thr581, it had no effect on the respective ATF2 or cJun phosphorylation levels, while the latter is inhibited by H89 (Figs. 4B and 5B, last lanes, respectively). This may seem as a discrepancy, since we are suggesting that both transcription factors constitute MSK1 substrates in our study. What should be taken into consideration though is the fact that MSK1 activity is controlled by multiple sites (Thr581, Ser360, Ser212, Ser376, Ser381, Ser750, Ser7552, Ser758) whose phosphorylation depends on upstream kinases activity or autophosphorylation [55]. Therefore, MSK1 can still be active while p38-MAPK is inactive. However, in the presence of H89, which blocks MSK1 activity, the latter cannot exert its action. To further substantiate MSK1 "interaction" with ATF2 and cJun, co-immunoprecipitation experiments were performed that verified our suggestion (Fig. 6). This observation is in accordance with other studies [56]. In particular, Zhu et al. [56] reported the direct interaction of ERKs with ATF2 and/or MSK1 in UVC-treated mouse epidermal JB6 cells.

ATF2 and cJun, being known AP-1 components [57], we predicted that they might exert their actions via increasing AP-1 transcription factor activity, leading to modifications in gene transcription. In particular, it is well established that ATF2 regulates gene expression by forming dimers with proteins containing basic region-leucine zipper domains, including cJun, and recognizing CRE or AP-1 sequences, implicated in cellular responses to stress [58]. Our hypothesis was confirmed since the time profile of AP-1 binding activity (Fig. 7A,B) accompanies those of ATF2 and cJun phosphorylation, thus activation. Indeed, among the various regulatory elements localized in the promoter 5′-flanking region of HOX-1, which control its gene expression, Alam and Den as well as Alam, have identified an AP-1 consensus site [59,60].

What is more, we observed AP-1 DNA binding activity to be markedly attenuated by SP600125 and H89, implicating JNKs and MSK1 in this response (Fig. 7C,D). This result is in accordance with reports of JNKs contributing to AP-1 activity via activation of ATF2 and cJun [61]. Furthermore, performing a large-scale activation profiling of genes whose promoters are bound and regulated by the AP-1 site binding cJun/ATF2 dimer,

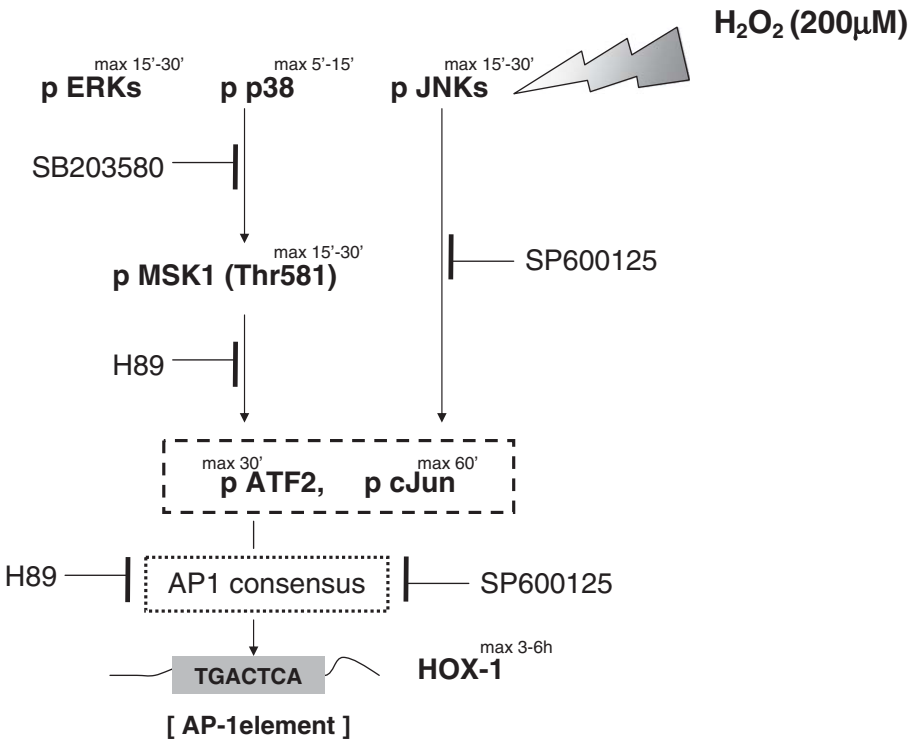

Fig. 8. A hypothetical model for regulation of HOX-1 transcriptional regulation in H_2O_2-treated H9c2 cardiomyoblasts. → activation, –/ inhibition.

Hayakawa et al. found among others, HOX-1 gene to be significantly differentially precipitated following genotoxic stress in BT474 cells [62].

On the other hand, the inhibitory effect of H89 on AP-1 binding activity could be attributed indirectly to ATF2 and cJun attenuated activity (Figs. 4B and 5B, last lanes), or directly to MSK1 responsive elements. The latter has been articulated by Darragh et al. who reported MSK1 responsive elements mapped to two AP-1-like elements in the nuclear orphan receptor Nur77 promoter, in TNF- or anisomycin-stimulated mouse embryonic fibroblasts [63].

5. Conclusions

Taken together, our results provide evidence concerning the signalling mechanism underlying HOX-1 mRNA stimulation by oxidative stress in H9c2 cells. This novel data marks the involvement of p38-MAPK, JNKs and MSK1 pathways in H_2O_2-induced HOX-1 transcriptional upregulation. What is more, our findings, which are summarized in Fig. 8, suggest that in our experimental setting, oxidative stress triggers the activation of two parallel pathways converging at ATF2 and cJun, modulating AP-1 binding activity. Based on the time-dependent sequential activation of all the components examined and since AP-1 elements have been reported in the rat HOX-1 promoter region [64,65], it is conceivable that JNKs and p38-MAPK/MSK1 mediate their effects via the pathways delineated in our study. Given the important role of HOX-1 in cardiovascular disorders, further studies are required to fully investigate the diversity and multiplicity of interactions between the signalling cascades leading to its regulation. A critical target of future investigation would also be the assessment of the specific physiological outcome of these complex interactions, aiming at potential therapeutic strategies enhancing enzymatic anti-oxidative defenses.

Acknowledgements

This work was funded by the PYTHAGORAS 1 grant (K.A. 70/3/7399).

References

[1] R. Tenhuen, H.S. Marver, R. Schmid, Proc. Natl. Acad. Sci. U. S. A. 61 (1968) 748.
[2] L.E. Otterbein, M.P. Soares, K. Yamashita, F.H. Bach, Trends Immunol. 24 (2003) 449.
[3] S. Shibahara, in: H. Fujita (Ed.), Regulation of Heme Protein Synthesis, Alpha Med Press, Dayton, OH, 1994, p. 103.
[4] I.A. Sammut, R. Foresti, J.E. Clark, D.J. Exon, M.J. Vesely, P. Sarathchandra, C.J. Green, R. Motterlini, Br. J. Pharmacol. 125 (1998) 1437.
[5] M. Suematsu, Y. Ishimura, Hepatology 31 (2000) 3.
[6] R. Stocker, Y. Yamamoto, A.F. Mcdonagh, A.N. Glazer, B.N. Ames, Science 235 (1987) 1043.
[7] C.D. Ferris, S.R. Jeffrey, A. Sawa, M. Takahashi, S.D. Brady, R.K. Barrow, S.A. Tysoe, H. Wolosker, D.E. Baranano, S. Dore, K.D. Poss, S.H. Snyder, Nat. Cell Biol. 3 (1999) 152.
[8] N. McCord, N. Engl. J. Med. 312 (1985) 159.
[9] R. Ferrari, L. Agnoletti, L. Comini, G. Gaia, T. Bachetti, A. Cargnoni, C. Ceconi, S. Curello, O. Visioli, Eur. Heart J. 19 (suppl B) (1998) B2.
[10] T. Ide, H. Tsutsui, S. Kinygawa, N. Suematsu, S. Hayashidani, K. Ichikawa, H. Utsumi, Y. Macida, K. Egashira, A. Taheshita, Circ. Res. 86 (2000) 152.
[11] S.M. Chen, Y.G. Li, D.M. Wang, Clin. Cardiol. 28 (2005) 197.

[12] K. Ishikawa, S. Kimura, A. Kobayashi, T. Sato, H. Matsumoto, Y. Ujie, K. Nakazato, M. Mitsugi, Y. Maruyama, Circ. J. 69 (2005) 617.
[13] A. Nakao, J.S. Neto, S. Kanno, D.B. Stolz, K. Kimizuka, F. Liu, F.H. Bach, T.R. Billiar, A.M. Choi, L.E. Otterbein, N. Murase, Am. J. Transp. 5 (2005) 282.
[14] B.W. Kimes, B.L. Brandt, Exp. Cell Res. 98 (1976) 367.
[15] C. Su, K. Chong, K. Edelstein, S. Lille, R. Khardori, C. Lai, Biochem. Biophys. Res. Commun. 265 (1999) 279.
[16] N. Turner, F. Xia, G. Azhar, X. Zhang, L. Liu, J. Wei, J. Mol. Cell. Cardiol. 30 (1998) 1789.
[17] H. Tanaka, K. Sakurai, K. Takahashi, Y. Fujimoto, J. Cell. Biochem. 89 (2003) 944.
[18] H. Han, H. Long, H. Wang, J. Wang, Y. Zhang, Z. Wang, Am. J. Physiol, Heart Circ. Physiol. 286 (2004) H2169.
[19] J.M. Kyriakis, J. Avruch, J. Biol. Chem. 271 (1996) 24313.
[20] M. Goedert, A. Cuenda, M. Craxton, R. Jakes, P. Cohen, EMBO J. 16 (1997) 3563.
[21] M.A. Bogoyevitch, Cardiovasc. Res. 45 (2000) 826.
[22] M. Deak, A. Clifton, J. Lucocq, D.R. Alessi, EMBO J. 17 (1998) 4426.
[23] S. Thomson, A. Clayton, C. Hazzalin, S. Rose, M.J. Baratt, L.C. Mahadevan, EMBO J. 18 (1999) 4779.
[24] S. Zhong, C. Jansen, Q.B. She, H. Goto, M. Inagaki, A.M. Bode, W.Y. Ma, Z. Dong, J. Biol. Chem. 276 (2001) 33213.
[25] L. Vermeulen, G. De Wilde, P. Van Damme, W. Vanden Berghe, G. Haegeman, EMBO J. 22 (2003) 1313.
[26] M.P. Delghandi, M. Johannessen, U. Moens, Cell. Signal. 17 (2005) 1343.
[27] J.A. Gustin, R. Pincheira, L.D. Mayo, O.N. Ozes, K.M. Kessler, M.R. Baerwald, C.K. Korgaonkar, D.B. Donner, Am. J. Physiol., Cell Physiol. 286 (2004) C547.
[28] A. Clerk, P.H. Sugden, Biochem. J. 325 (1997) 801.
[29] T.J. Kemp, H. Causton, A. Clerk, Biochem. Biophys. Res. Commun. 307 (2003) 416.
[30] T. Markou, M. Hadzopoulou-Cladaras, A. Lazou, J. Mol. Cell. Cardiol. 37 (2004) 1001.
[31] A. Clerk, J.G. Harrison, C.S. Long, P.H. Sugden, J. Mol. Cell. Cardiol. 31 (1999) 2087.
[32] T. Herdegen, J.D. Leah, Brain Res. Rev. 28 (1998) 370.
[33] S. Hayashi, R. Takamiya, T. Yamaguchi, K. Matsumoto, S.T. Tojo, T. Tamatani, M. Kitajima, N. Makino, Y. Ishimura, M. Suematsu, Circ. Res. 85 (1999) 663.
[34] J.A. Araujo, L. Meng, A. Tward, W.W. Hancock, Y. Zhai, A. Lee, K. Ishikawa, S. Iyer, R. Buelow, R.W. Busuttil, D.M. Shih, A.J. Lusis, J.W. Kupiec, J. Immunol. 171 (2003) 1572.
[35] R. Motterlini, Cell. Mol. Biol. (Noisy-le-grand) 51 (2005) 343.
[36] T. Lee, C. Chang, Y. Zhu, J. Shyy, Circulation 110 (2004) 1296.
[37] N. Wijayanti, T. Kietzmann, S. Immenschuh, J. Biol. Chem. 280 (2005) 21820.
[38] W. Ning, R. Song, C. Li, E. Park, A. Mohsenon, A. Choi, M. Choi, Am. J. Physiol., Lung cell. mol. physiol. 283 (2002) L1094.
[39] R. Kacimi, J. Chentoufi, N. Honbo, C.S. Long, J. Karliner, Cardiovasc. Res. 46 (2000) 139.
[40] T. Oguro, M. Hayashi, S. Nakajo, S. Numazawa, T. Yoshida, J. Pharmacol. Exp. Ther. 287 (1998) 773.
[41] X. Zhang, E.L. Bedard, R. Potter, R. Zhong, J. Alam, A. Choi, P. Lee, Am. J. Physiol., Lung Cell. Mol. Physiol. 283 (2002) L815.
[42] K. Chen, M.D. Maines, Cell. Mol. Biol. 46 (2000) 609.
[43] S. Keysell, R. Tyrrell, Proc. Natl. Acad. Sci. U. S. A. 86 (1989) 99.
[44] A. Clerk, A. Michael, P.H. Sugden, Biochem. J. 333 (1998) 581.
[45] S. Rakhit, C.J. Clark, C.T. O'Shaughnessy, B.J. Morris, Mol. Pharmacol. 67 (2004) 1158.
[46] Y. Zhang, G. Liu, Z. Dong, J. Biol. Chem. 276 (2001) 42534.
[47] K.M. Weber, M.A. Smith, H.G. Lee, P.L. Harris, P. Moreira, G. Perry, X. Zhu, J. Neurosci. Res. 79 (2005) 554.
[48] F. Romano, C. Chiarenza, F. Palombi, A. Filippini, F. Padula, E. Ziparo, P. De Cesaris, J. Cell. Physiol. (2005) PMID: 162703525.
[49] M. Nomura, A. Kaji, W.Y. Ma, S. Zhong, G. Liu, G.T. Bowden, K.I. Miyamoto, Z. Dong, J. Biol. Chem. 276 (2001) 25558.
[50] J. Darragh, A. Soloaga, V.A. Beardmore, A.D. Wingate, G.R. Wiggin, M. Peggie, J.S. Arthur, Biochem. J. 390 (2005) 749.
[51] R. Hokari, H. Lee, S.C. Crawley, S.C. Yang, J.R. Gum, S. Miura, Y.S. Kim, Am. J. Physiol.: Gasterointest. Liver Physiol. 289 (2005) G949.
[52] G. Liu, Y. Zhang, A.M. Bode, W.Y. Ma, Z. Dong, J. Biol. Chem. 277 (2002) 8810.
[53] S. Kurata, J. Biol. Chem. 275 (2000) 23413.
[54] T. Buschmann, Z. Yin, A. Bhoumik, Z. Ronai, J. Biol. Chem. 275 (2000) 16590.
[55] C.E. Mccoy, D.G. Campbell, M. Deak, G.B. Bloomberg, J.S. Arthur, Biochem. J. 387 (2005) 507.
[56] F. Zhu, Y. Zhang, A. Bode, Z. Dong, Carcinogenesis 25 (2004) 1847.
[57] K.K. Yamamoto, G.A. Gonzalez, W.D. Biggs, M.R. Montminy, Nature 334 (1988) 494.
[58] T.W. Hai, F. Liu, W.J. Coukos, M.R. Green, Genes Dev. 3 (1989) 2083.
[59] J. Alam, Z. Den, J. Biol. Chem. 267 (1992) 21894.
[60] A. Alam, J. Biol. Chem. 269 (1994) 25049.
[61] P. Yuan, G. Chen, H. Manji, J. Neurochem. 73 (1999) 2299.
[62] J. Hayakawa, S. Mittal, Y. Wang, K.S. Korkmaz, E. Adamson, C. English, M. Omichi, M. McClelland, D. Mercolla, Mol. Cell 16 (2004) 521.
[63] J. Darragh, A. Soloaga, V.A. Beardmore, A.D. Wingate, G.R. Wiggin, M. Peggie, J.S. Arthur, Biochem. J. 390 (2005) 749.
[64] S. Kurata, H. Nakajima, Exp. Cell Res. 1911 (1990) 89.
[65] G. Wu, J. Maria-Garcia, T.B. Rogers, E.G. Lakatta, X. Long, J. Card. Fail. 10 (2004) 519.